The role of osmotic polysorbitol-based transporter in RNAi silencing via caveolae-mediated endocytosis and COX-2 expression

Mohammad Ariful Islam [a,b,c], Ji-Young Shin [d], Jannatul Firdous [a,b], Tae-Eun Park [a,c], Yun-Jaie Choi [a,c], Myung-Haing Cho [d,e], Cheol-Heui Yun [a,b,c,**], Chong-Su Cho [a,c,*]

[a] Department of Agricultural Biotechnology, Seoul National University, Seoul 151-921, Republic of Korea
[b] Center for Agricultural Biomaterials, Seoul National University, Seoul 151-742, Republic of Korea
[c] Research Institute for Agriculture and Life Sciences, Seoul National University, Seoul 151-921, Republic of Korea
[d] Laboratory of Toxicology, College of Veterinary Medicine, Seoul National University, Seoul 151-742, Republic of Korea
[e] Department of Nanofusion Technology, Graduate School of Convergence Science and Technology, Seoul National University, Seoul 151-742, Republic of Korea

ARTICLE INFO

ABSTRACT

Polymeric diversity allows us to design gene carriers as an alternative to viral vectors, control cellular uptake, target intracellular molecules, and improve transfection and silencing capacity. Recently, we developed a polysorbitol-based osmotically active transporter (PSOAT), which exhibits several interesting mechanisms to accelerate gene delivery into cells. Herein, we report the efficacy of using the PSOAT system for small interfering RNA (siRNA) delivery and its specific mechanism for cellular uptake to accelerate targeted gene silencing. We found that PSOAT functioned via a caveolae-mediated uptake mechanism due to hyperosmotic activity of the transporter. Moreover, this selective caveolae-mediated endocytosis of the polyplexes (PSOAT/siRNA) was regulated coincidently with the expression of caveolin (Cav)-1 and cyclooxygenase (COX)-2. Interestingly, COX-2 expression decreased dramatically over time due to degradation by the constant expression of Cav-1, as confirmed by high COX-2 expression after the inhibition of Cav-1, suggesting that PSOAT-mediated induction of Cav-1 directly influenced the selective caveolae-mediated endocytosis of the polyplexes. Furthermore, COX-2 expression was involved in the initial phase for rapid caveolae endocytic uptake of the particles synergistically with Cav-1, resulting in accelerated PSOAT-mediated target gene silencing.

© 2012 Elsevier Ltd. All rights reserved.

1. Introduction

Since the discovery of RNA interference (RNAi) by Fire and Mello in 1998, for which they received the Nobel Prize, the concept and its applications for effective and targeted gene silencing have been explored considerably [1]. Small interfering RNAs (siRNAs) were introduced in early 2001 [2,3] and thereafter, the first experimental approach for a gene silencing strategy targeting hepatitis C in mice was achieved using siRNA [4]. Since the remarkable breakthrough, experts in this field have made considerable advancements in siRNA therapeutics against various diseases including viral infections and cancers [5–7]. However, this exciting and promising approach has not yet been translated into the clinical side, owing to several limitations. The most significant challenges are the relatively large size (~13 kDa) and negative charges of siRNA molecules, together with their susceptibility to degradation by endogenous enzymes [6,7]. Although naked siRNAs have been shown to be effective in a few physiological settings and applications [8,9], an improved delivery system to facilitate siRNA transfection is required in most body tissues because naked siRNAs are unable to cross cellular membranes freely due to their strong anionic charges. Thus, an effective delivery system for siRNA remains a challenge and the most critical barrier between siRNA technology and its therapeutic application. At present, numerous gene therapies in clinical trials use recombinant viral vectors due to their excellent transfection ability; however, safety issues have halted their further advancement. Therefore, to achieve therapeutic advantages using siRNA, not only clinical safety but also an effective delivery system must be in place; non-viral polymeric carriers could be the best, most effective alternative.

Cationic polyethylenimine (PEI), one of the most widely investigated polymers, has been used as a non-viral gene carrier. However, PEI-mediated gene transfer may cause severe cellular

* Corresponding author. Department of Agricultural Biotechnology, Seoul National University, Seoul 151-921, Republic of Korea. Tel.: +82 2 880 4868; fax: +82 2 875 2494.
** Corresponding author. Department of Agricultural Biotechnology, Seoul National University, Seoul 151-921, Republic of Korea. Tel.: +82 2 880 4802.
E-mail addresses: cyun@snu.ac.kr (C.-H. Yun), chocs@snu.ac.kr (C.-S. Cho).

toxicity due to its non-degradable nature and has a low transfection capability relative to viral vectors, major drawbacks hindering its clinical application [10]. Hence, the modification of PEI using degradable cross-linkers has been investigated extensively to introduce degradable properties to improve its cellular viability [10]. Recently, we developed a class of gene transporter, the polysorbitol-based osmotically active transporter (PSOAT), prepared from sorbitol dimethacrylate (SDM) and low-molecular-weight linear polyethylenimine (LMW LPEI), which exhibits accelerated gene transfer capability. The transfection activity of PSOAT is greatly hampered by COX-2 and vacuolar-type proton ATPase-specific inhibitors but is enhanced by osmotic activity and many hydroxyl groups contained in the polysorbitol chain of the transporter [10]. Although hydroxyl groups of polymers have been reported to reduce gene transfection efficiency [11,12], interestingly, PSOAT shows an accelerated gene transfer capability despite its many hydroxyl groups [10]. The osmotic PSOAT exploits a transporter mechanism related with its polysorbitol backbone, which enhances cellular internalization. However, the precise cellular uptake mechanism, which is essential for its use as a delivery tool for therapeutic agents such as siRNA, remains unknown.

A potential strategy for improving gene delivery by non-viral carriers is to target a particular cellular uptake process that is closely related with intracellular fate [13,14]. The mechanism for the cellular uptake of nanoparticles has been suggested to be either clathrin-dependent or clathrin-independent endocytosis [15]. Clathrin-dependent cellular uptake follows the classic endocytic pathway, which cannot avoid the fusion of endosomes carrying

a target molecule(s) to a lysosome, resulting in enzymatic degradation. On the other hand, clathrin-independent, particularly caveolae-mediated endocytosis leads to the transport of endocytosed materials toward the non-acidic and non-digestive route without fusion to a lysosome [16,17]. Several reports have also demonstrated the advantages of caveolae-mediated cellular uptake [18—20]. These studies have emphasized the importance of proper design and the development of non-viral gene vectors targeting caveolae-dependent uptake to achieve effective intracellular processing for the expected gene expression profile. Moreover, other recent reports emphasized on designing nanoparticles and their translocations through cellular membrane using computer simulation strategy which may provide new ideas and concept for future experimental nanoparticle design and their potential use in drug delivery system [21—23].

It is interesting to note that hypertonic exposure of cells can be used to selectively stimulate the caveolae-mediated endocytic pathway by downregulating clathrin-dependent endocytosis and fluid-phase uptake [24]. Caveolae endocytosis involves the expression of caveolin (Cav), especially Cav-1, a major component of caveolae formation, which could stabilize caveolae receptors and the receptors at the plasma membrane outside of caveolae that affect the caveolae-mediated endocytosis mechanism [25—27]. This notion is further supported by the fact that cells under osmotic stress induce Cav-1 phosphorylation via Src-kinase activity during the process of budding and pinching off from the plasma membrane [28]. Thus, it appears that Cav-1 expression has a direct functional mechanism for caveolae endocytosis under osmotic
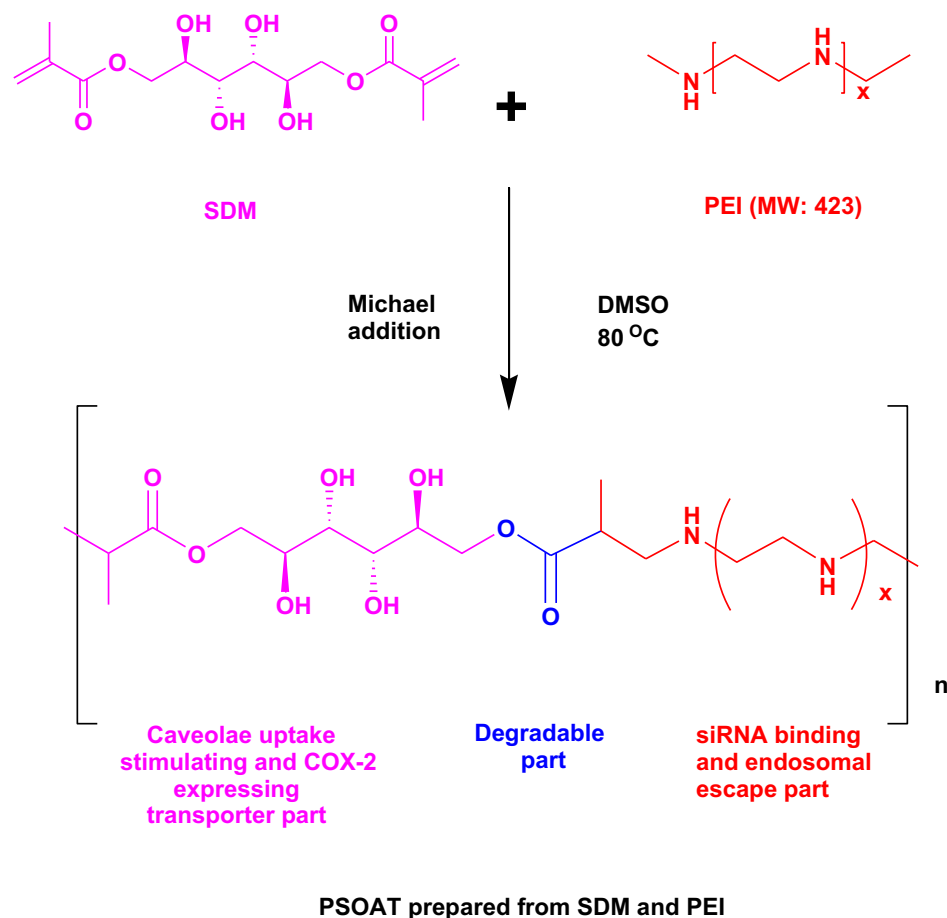

PSOAT prepared from SDM and PEI

Fig. 1. Proposed reaction scheme for the synthesis of PSOAT from SDM and PEI. PSOAT was prepared through a Michael addition reaction in DMSO at 80 °C. Different colors indicate different functional parts of PSOAT. (For interpretation of the references to colour in this figure legend, the reader is referred to the web version of this article.)

stimuli. Moreover, hyperosmotic conditions induce COX-2 expression by activating several osmosensing molecules and regulate COX-2 activity with osmolyte-dependent cellular adaptation [29,30]. Cells with high COX-2 expression show more cellular uptake than cells with low COX-2 expression, indicating the importance of COX-2 expression in the uptake mechanism [31]. Because caveolae-mediated endocytic transport and its signal transduction are tightly linked with caveolae [32], COX-2 expression along with Cav-1 could affect caveolae-mediated endocytosis. This indicates that non-viral carriers with hyperosmotic properties could be promising tools for triggering the cellular entry of genes through a selective route. Therefore, we hypothesized that this could be useful for the efficient delivery of siRNA using PSOAT to achieve effective silencing.

In this study, we investigated the efficacy of using PSOAT as a siRNA transporter system for effective target gene silencing. Osteopontin (OPN) siRNA was used as a model for therapeutic siRNA because it plays an important role in tumor angiogenesis [33,34]. Considering the importance of OPN suppression, the PSOAT system was applied to deliver OPN siRNA (siOPN) to downregulate its expression. Importantly, the mechanism of PSOAT was investigated to define the specificity of cellular uptake and gene silencing efficacy.

2. Materials and methods

2.1. Materials

Branched PEI (MW: 25 kDa), linear PEI (LPEI, MW: 423 Da), and 3-(4, 5-dimethyl thioazol-2-yl)-2, 5-diphenyl tetrazolium bromide (MTT) reagent were purchased from Sigma−Aldrich (St. Louis, MO, USA). Sorbitol dimethacrylate (SDM) was purchased from Monomer−Polymer & Dajac Labs, Inc. (Trevose, PA, USA). A non-targeted scrambled siRNA (siScr) was used for gel electrophoresis, TEM, DLS, cell viability, and immunofluorescence experiments, whereas other siRNAs for silencing luciferase (siLuc), GFP (siGFP), and OPN (siOPN) were used for specific targeting (Table S1). The siRNAs were purchased from Genolution Pharmaceuticals, Inc. (Seoul, South Korea).

2.2. Synthesis of PSOAT

PSOAT was synthesized via a Michael addition reaction between SDM and low-molecular-weight LPEI in anhydrous dimethyl sulfoxide (DMSO) at 80 °C, as depicted in Fig. 1 [10]. To measure osmolarity (mOsm), PSOAT was dissolved in 10% serum containing media at various polysorbitol percentages (1, 3, and 5 wt%) and osmolarity was measured using an automatic cryoscopic osmometer (OSMOMAT® 030-D, Gonotec, Germany). Media containing 10% serum was used as the control.

2.3. Complexation, protection, and release of siRNA

The ability of the transporter to complex with siRNA was examined by gel retardation assay according to N/P and weight ratios. Briefly, PSOAT/siRNA (1 μg) complexes were prepared at various N/P ratios from 1 to 30 and weight ratios from 0.1 to 3. The final volume of the complexes for each sample was 15 μL, including agarose gel loading dye mixture (Biosesang, Korea) and ethidium bromide (EtBr, 1 μL/ sample). The complexes were loaded onto an agarose gel (3%) and run at 100 V for 40 min with Tris/borate/EDTA (TBE) buffer. Finally, siRNA retardation was observed under ultraviolet illumination. The protection and release of siRNA was also investigated using gel electrophoresis. Briefly, PSOAT/siRNA complexes (N/P 10) were incubated at 37 °C for 30 min with two different RNase concentrations (0.1 and 1.0 μg/ μL). Then, 4 μL EDTA was added and incubated for additional 30 min at room temperature (RT) for RNase inactivation. Finally, 5 μL 1% sodium dodecyl sulfate (SDS) dissolved in distilled water was mixed and incubated for 2 h at RT. Electrophoresis was performed in a 3% agarose gel with TBE running buffer at 100 V for 40 min.

2.4. Morphology, size, and surface charge of PSOAT/siRNA complexes

The morphology of PSOAT/siRNA complexes (N/P 10) was observed by transmission electron microscopy (TEM) (LIBRA 120, Carl Zeiss, Germany). Particle size and surface charge of the complexes were measured using a dynamic light scattering spectrophotometer (DLS 8000, Otsuka Electronics, Osaka, Japan), as described previously [10].

2.5. Cell culture and cytotoxicity of PSOAT/siRNA complexes

A549 human lung adenocarcinoma cells were maintained in Roswell Park Memorial Institute (RPMI)-1640 culture medium containing 10% heat-inactivated fetal bovine serum (FBS, Hyclone, Logan, UT, USA) with 1% penicillin/streptomycin at 37 °C with 5% CO_2. The cytotoxicity of PSOAT/siRNA complexes was evaluated in A549 cells at various N/P ratios (5, 10 and 20) for 48 and 72 h and compared against the standard polymeric carrier (PEI 25K/siRNA complexes) by MTT assay, as described previously [10].

2.6. Silencing studies

2.6.1. GFP silencing

A549 cells were first transfected with Lipofectamine™/tGFP complex according to the manufacturer's protocol to express stable turboGFP (tGFP) protein. GFP-expressing A549 cells were then transfected with PSOAT/siGFP or siScr complexes (N/P 10) in serum free media containing siRNA concentrations of 100 pmol/L. The media were changed after 4 h with complete RPMI-1640 media. After 36 h of incubation, the silencing efficiency was measured by flow cytometry (BD Biosciences, San Jose, CA, USA), as well as observation using fluorescent microscopy (Carl Zeiss, Axiovert40 CFL, Germany). The percent tGFP silencing with PSOAT/siGFP complexes was calculated after normalizing the results with respective mock-treated cells and then compared to the silencing of the PSOAT/siScr-treated group.

2.6.2. Silencing of luciferase activity

Luciferase-expressing A549 cells were transfected with PSOAT/siLuc or siScr complexes (N/P 10) in serum-free media prepared containing siRNA concentrations of 100 pmol/L and incubated at 37 °C with 5% CO_2. Similarly, PEI 25K/siLuc or siScr complexes were prepared (N/P 5) and the cells were transfected. After 4 h, the serum free media were replaced with complete media and further incubated for 48 h. Finally, luciferase expression was measured by luciferase assay (Promega, Madison, WI, USA) using a chemiluminometer (Autolumat, LB953; EG&G Berthold, Germany) and normalized with the protein concentration in the cell extract determined using a BCA protein assay kit (Pierce Biotechnology, Rockford, IL, USA). The luciferase silencing efficiency was calculated as the relative percentage of luciferase activity to control cells without siRNA treatment.

2.6.3. Silencing of OPN expression

2.6.3.1. Quantitative reverse transcription−polymerase chain reaction (RT-qPCR). RT-qPCR was performed to examine the silencing of OPN expression at the mRNA level following PSOAT-mediated delivery of siOPN in A549 cells. The cells were seeded at a density of 3×10^5 cells/well in a 6-well plate. Cells (80% confluence) were then transfected with PSOAT/siOPN complexes (N/P 10). The cells were harvested after 24 h, and total RNA was isolated using the QuickGene RNA kit (Fujifilm, Tokyo, Japan). Then, cDNA was synthesized using the Finnzymes cDNA synthesis kit with MMLV reverse transcriptase (Thermo Fisher Scientific Inc., Vantaa, Finland) and random primer. PCR mixtures were prepared with $2 \times$ Prime Q-Mastermix containing $2 \times$ SYBR® Green I (Genet Bio, Nonsan, Korea) according to the manufacturer's protocol. RT-qPCR was performed in quadruplicate for each group with hOPN and hGAPDH primers (Table S2) using a C1000 Thermal Cycler (BioRad, CA, USA) starting with 10 min of pre-incubation at 95 °C followed by 40 amplification cycles with an annealing temperature at 52 °C. The fluorescent signal intensities were measured and analyzed using C1000Manager Software (BioRad, Hercules, CA, USA).

2.6.3.2. Western blot analysis. A549 cells were seeded in a 75-mm flask and allowed to grow to about 80% confluence prior to transfection with PSOAT/siOPN complexes (N/P 10). The cells were then harvested after 48 h and lysed with $5 \times$ lysis buffer (Promega). Protein concentrations were measured using a Bradford kit (BioRad). Equal amounts of protein (25 μg) were separated by SDS-PAGE, transferred to nitrocellulose membrane, and then pre-blocked with 5% skim milk for 1 h at RT. After washing, the membrane was incubated overnight at 4 °C with anti-OPN (Santa Cruz Biotechnology Inc., Santa Cruz, CA, USA) and anti-GAPDH (Abfrontier, Seoul, Korea) antibodies diluted to 1:500. Then, the secondary antibodies conjugated with HRP (Invitrogen, Carlsbad, CA, USA) were applied according to the manufacturer's protocols. Bands of interest were captured using a luminescent image analyzer LAS-3000 (Fujifilm, Tokyo, Japan) and quantified using Multi Gauge (Fujifilm).

2.7. Mechanistic studies of PSOAT on accelerated gene silencing

2.7.1. Inhibition of cellular uptake to determine uptake selectivity

Various cellular uptake inhibitors such as genistein (GE), methyl-β-cyclodextrin (MβC), chlorpromazine (CH), and wortmannin (Wor) were used. First, GE and Wor were dissolved in cell culture-grade DMSO (Sigma), and CH and MβC were dissolved in DNase−RNase free distilled water (GIBCO, ultraPURE™). The inhibitors were further diluted to various concentrations with serum free media and used to treat luciferase-expressing A549 cells at 37 °C with 5% CO_2 for 1 h. Then, the cells were transfected with PSOAT/siLuc (N/P 10) and PEI 25K/siLuc (N/P 5) complexes prepared in serum free media. After 4 h, the media were replaced with fresh complete media and the cells were incubated for an additional 48 h. Finally, luciferase assay was performed as described to assess the differences in luciferase silencing efficacy of the carrier in the presence of various inhibitors after being normalized with the luciferase activity of control cells without siRNA treatment.
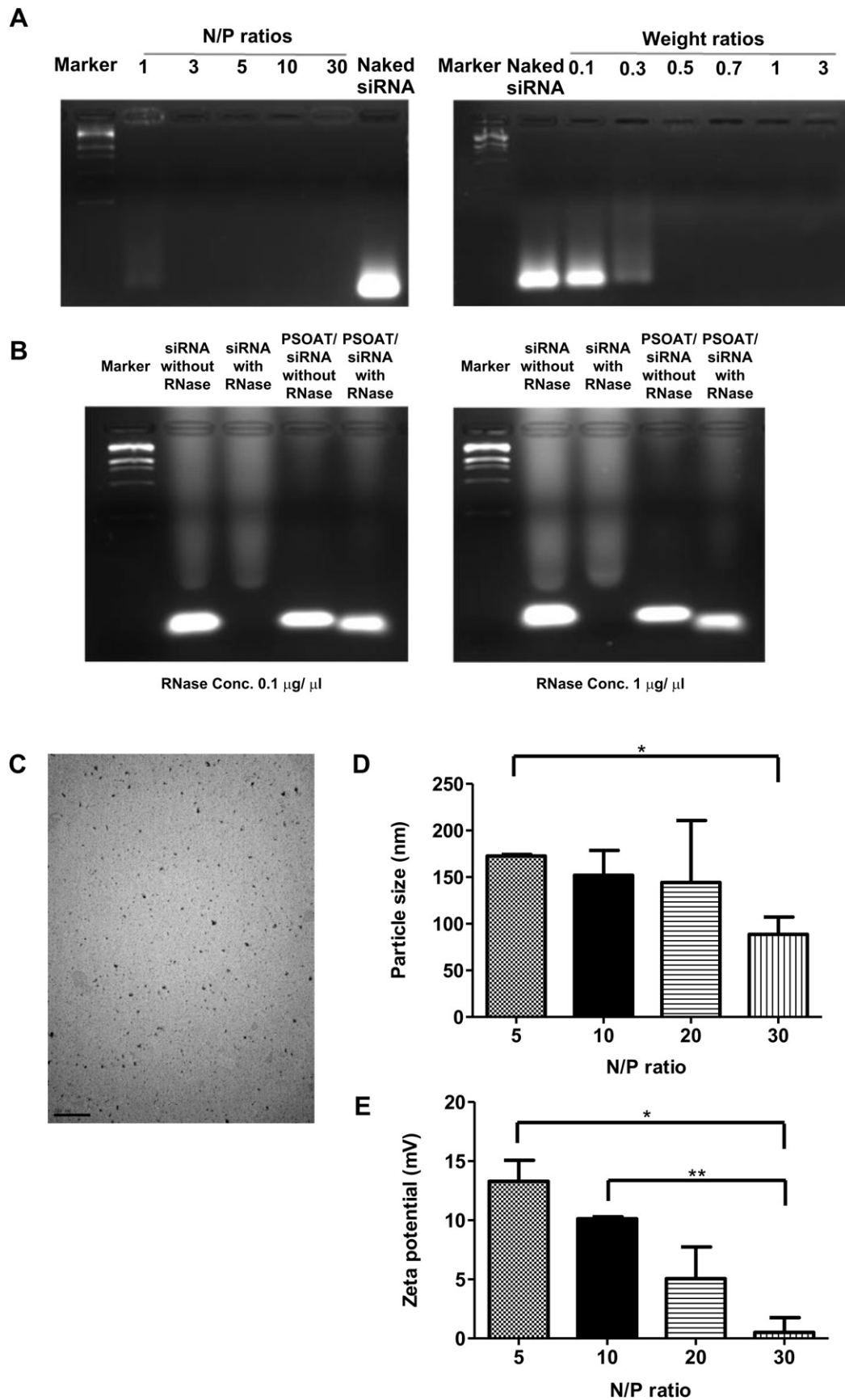
Fig. 2. Characterization of PSOAT/siRNA complexes. (A) Agarose gel electrophoresis of PSOAT/siRNA complexes at various N/P ratios ranging from 1 to 30, and weight ratios ranging from 0.1 to 3. One microgram of siRNA was used to complex with PSOAT. (B) Naked siRNA and PSOAT/siRNA complexes (N/P 10) were incubated with or without RNase for 30 min at 37 °C with shaking. Two different RNase concentrations (0.1 and 1.0 μg/μL) were used to examine siRNA protection from RNase degradation. SDS (1%) was used to release siRNA from PSOAT/siRNA complexes. (C) TEM images of PSOAT/siRNA complexes (N/P 10). The bar denotes 200 nm. (D) Particle sizes, and (E) Zeta potentials were measured at various N/P ratios from 5 to 30 ($n = 3$, error bar represents SD) (*$P < 0.05$, **$P < 0.01$, one-way ANOVA).

2.7.2. Effect of COX-2 inhibition on PSOAT-mediated silencing

SC236, a COX-2 specific inhibitor, has been reported to inhibit the uptake of organic osmolytes (such as sorbitol) into cells [29]. In light of this fact, PSOAT-mediated gene silencing was investigated using SC236 to inhibit the osmotic activity of PSOAT and PSOAT-mediated induction of COX-2 expression in A549 cells. Luciferase-expressing A549 cells (80% confluence) were treated with SC236 (dissolved in DMSO and diluted in serum free RPMI-1640) at various concentrations and incubated for 1 h. Then, PSOAT/siLuc (N/P 10) and PEI 25K/siLuc (N/P 5) complexes were prepared in serum free media and transfected to cells in the presence of the inhibitor. Luciferase assay was performed as described above.

2.7.3. Involvement of Cav-1 and COX-2 expression in PSOAT-mediated gene silencing

To address the involvement of Cav-1 and COX-2 expression in PSOAT-mediated gene silencing, A549 cells were transfected with PSOAT/siRNA complexes and the expression of Cav-1 and COX-2 were observed separately at various time points (15, 30, 60, and 120 min post-transfection) by immunofluorescence assay using image restoration microscopy (IRM, DeltaVision RT, USA). Briefly, A549 cells, cultured on gelatin (0.1%)-coated glass slides, were transfected with PSOAT/siRNA complexes and maintained under standard incubation conditions for 15, 30, 60, and 120 min. Untreated cells were used as a control. At each time interval, the cells were washed with phosphate-buffered saline (PBS) and primarily fixed with 4% paraformaldehyde (PFA) for 10 min at 37 °C, followed by a final fixation with a mixture of 100% methanol and acetone (1:1) for 10 min at −20 °C. The cells were then washed twice with PBS and blocked with 10% FBS for 1 h at 37 °C. Polyclonal rabbit Cav-1 (1:50) or COX-2 (1:50) IgG antibodies (Santa Cruz Biochemicals) diluted in blocking solution were added to the respective sample and incubated for 1 h. The samples were then washed five times (5 min each) with PBS and then treated for 30 min with the anti-rabbit secondary antibodies conjugated with fluorescein isothiocyanate (FITC) for Cav-1 and rhodamine isothiocyanate (RITC) for COX-2. After five additional washes, the cells were mounted with DAPI containing fluoroshield solution (10 μL per sample) for tracking the nucleus and to protect fluorescence intensity. Finally, the samples were sealed with cover glass (Marienfeld, Germany) and visualized using IRM at RT. At least 1000 cells with typical morphology per sample were tested.

Furthermore, colocalization of Cav-1 and COX-2 followed by PSOAT/siRNA transfection was examined in the absence or presence of caveolae-disrupting agent, MβC and/or COX-2-specific inhibitor, SC236 in A549 cells. Briefly, A549 cells were incubated with MβC (3 mg/mL) and/or SC236 (20 μM) for 1 h and transfected with PSOAT/siRNA complexes in the presence of the inhibitors for 30 or 120 min. The cells were fixed and blocked as described above, and then treated with the monoclonal mouse anti-human Cav-1 antibody (Abcam®, Cambridge, CB4 0FL, UK) and polyclonal rabbit anti-human COX-2 antibody (Santa Cruz Biochemicals) followed by treatment with anti-mouse FITC antibody and anti-rabbit RITC antibody, respectively. At least 1000 cells with typical morphology per sample were examined through IRM. The colocalization intensity was analyzed quantitatively using ImageJ software (NIH, USA) and plotted as the mean pixel value.

3. Results and discussion

3.1. Characterization of PSOAT/siRNA complexes

The ultimate goal of studying PSOAT was to develop an efficient carrier system for therapeutic agents such as siRNA. It is important to note that siRNA should be effectively condensed for efficient delivery. However, most polymers are insufficient due to the high stiffness and low charge density of siRNA, which limit its nanocomplex-forming ability, especially for intracellular uptake through an endocytic pathway [35]. To investigate the complex forming ability of the PSOAT system with siRNA, an agarose gel electrophoresis assay was performed at various N/P ratios (1, 3, 5, 10, and 30). The complex was further confirmed at different weight ratios of PSOAT/siRNA complexes (0.1, 0.3, 0.5, 0.7, 1, and 3). The results showed that PSOAT was remarkably effective at forming complexes of siRNA at a minimal N/P ratio of 3 and weight ratio of 0.5 (Fig. 2A), indicating its excellent siRNA condensation ability.

Next, we tested the protection of PSOAT-complexed siRNA from RNase at concentrations of 0.1 and 1.0 μg/μL. There was complete and comprehensive protection of siRNA from RNase when complexed with PSOAT, whereas the naked siRNA was degraded even at 0.1 μg/μL RNase, suggesting that the effective and stable siRNA complexation by PSOAT protects against degradation (Fig. 2B). This protection ability of PSOAT complexed with siRNA satisfied the first requirement for the effective transportation of siRNA into the cells.
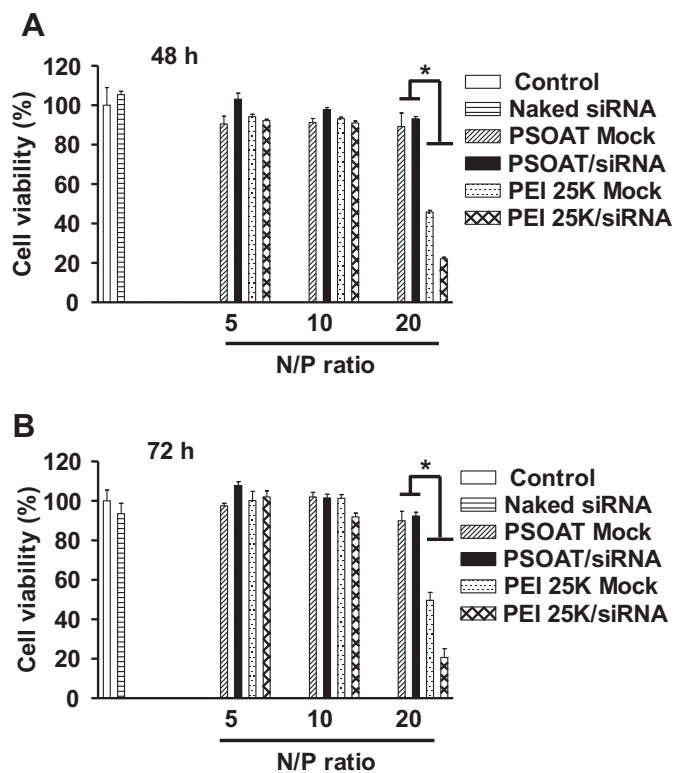
Fig. 3. Cytotoxicity of PSOAT/siRNA and PEI 25K/siRNA complexes at various N/P ratios in A549 cells. Cells were transfected with PSOAT/siRNA and PEI 25K/siRNA complexes at various N/P ratios and the cytotoxicity of the complexes was evaluated after (A) 48 and (B) 72 h ($n = 3$, error bar represents SD) (*$P < 0.05$, one-way ANOVA).

The size, surface charge, and morphology of non-viral gene carriers are important because they influence the biological fate, toxicity, and effectiveness of the system for improving cellular uptake and *in vivo* distribution [36]. A representative morphology of PSOAT/siRNA complexes displayed by TEM analysis is presented in Fig. 2C. The particles were nanosized, spherical compact, and uniformly distributed. The size of PSOAT/siRNA complexes was measured at different N/P ratios from 5 to 30 by DLS. For all N/P ratios, the particles were <200 nm (Fig. 2D), which could be highly efficient for effective endocytosis and cellular internalization. The zeta potential of PSOAT/siRNA complexes decreased as the N/P ratio increased, as expected (Fig. 2E) because the shielding effect of the hydroxyl groups of PSOAT is high. It has been reported that the shielding effect of hydroxyl groups can be reduced by increasing the amine groups [11], suggesting that the effect of hydroxyl groups on the surface charge of nanoparticles depends on the density of the amine group. PSOAT is composed of LPEI with a low molecular weight (423 Da), which has a low density of amines. This is why the zeta potentials decreased dramatically as the N/P ratio increased. The lower zeta potential of PSOAT/siRNA complexes is likely better for reducing the charge-mediated toxicity of the particles without affecting the cellular internalization of siRNA through the PSOAT system.

3.2. Cytotoxicity assay in vitro

Cytotoxicity must be overcome to realize the efficient and safe delivery of siRNA. We examined the toxicity of PSOAT in a complex form with siRNA or alone (as a mock) and compared them to the respective complexes or mock of PEI 25K in A549 cells at various N/P ratios (5, 10, and 20) at 48 and 72 h post-transfection by MTT

assay. The PSOAT/siRNA complexes and the mock both exhibited >90% cell viabilities, even at the highest N/P ratio of 20 (Fig. 3). In contrast, the cell viability of PEI 25K/siRNA complexes declined markedly to around 20% at N/P ratio of 20. These results suggest that PSOAT is a safe carrier system for siRNA delivery compared to the standard PEI 25K. PEI would impair cell membrane function by aggregating on the cell surface due to its non-degradative nature, and thus exhibit high toxicity [37]. The toxicity of PEI also depends on its molecular weight and the type of PEI molecule, as the low-molecular-weight LPEIs are less toxic than their high-molecular-weight and branched counterparts. Moreover, the inclusion of hydroxyl groups on polycationic gene carriers may help reduce their toxicity [11]. On the other hand, the degradability of poly-mers reduces their cytotoxic effects. Indeed, the PSOAT system possesses degradability owing to its degradable ester linkages [10]. Hence, the combination of low (MW) LPEI, presence of

Table 1
Measurement of osmolarity (mOsm) of PSOAT.

Groups	Sorbitol/polysorbitol wt (%)	Osmolarity (mOsm)
RPMI + 10% FBS	0	273
D-Sorbitol	1	334
	3	449
	5	598
	10	879
PSOAT	1	281
	3	375
	5	481

abundant hydroxyl groups, and degradability of PSOAT contributes to the reduced toxicity and improved safety of this siRNA trans-porter system.

Recently, alkane-modified low MW PEI (MW: 600) was reported for siRNA delivery, where the PEI was used as a cationic backbone and
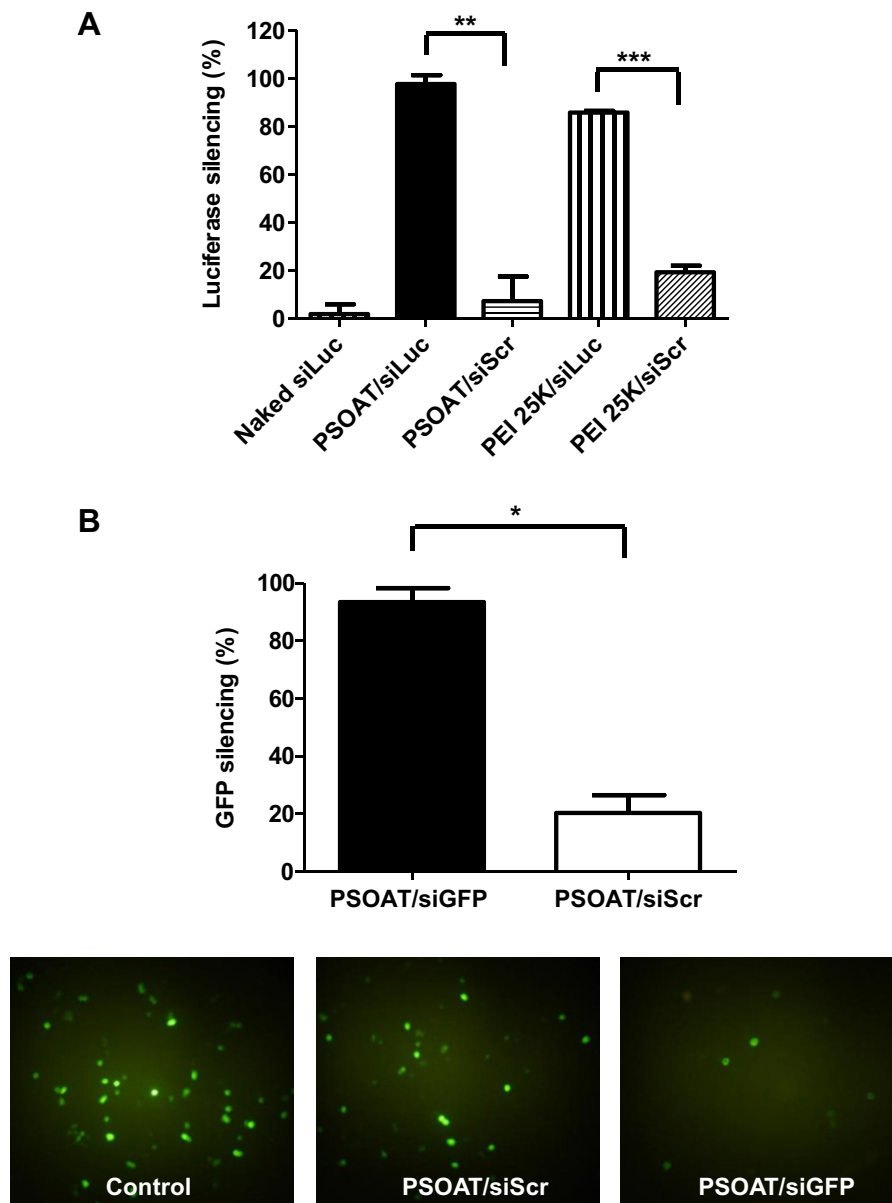

Fig. 4. Silencing efficacy of PSOAT/siLuc and PSOAT/siGFP in A549 cells. Luciferase- or GFP-expressing A549 cells at 80% confluence were transfected with the polymer/siRNA complexes and examined for luciferase or GFP silencing efficacy. (A) Luciferase silencing by PSOAT/siLuc and PEI 25K/siLuc complexes compared to the respective scrambled siRNA (siScr) group. (B) GFP silencing efficacy of PSOAT/siGFP complexes compared to the respective siScr group at a siRNA concentration of 100 pmol/L ($n = 3$, error bar represents SD) (*$P < 0.05$; **$P < 0.01$; ***$P < 0.001$, one-way ANOVA) and fluorescent images of control, PSOAT/siScr- and PSOAT/siGFP-treated A549 cells (magnification: 10×).

to conjugate with various number of lipid tails [38]. This polymer–lipid hybrid was capable of complexing siRNA and silenced genes specifically with low cytotoxicity because of the lipid-tailored modification. Therefore, modification of PEI, especially with degradable and non-toxic crosslinkers is a promising strategy to reduce PEI-mediated toxicity, where the PSOAT is showing excellent tolerability to cells owing to have suitable structural composition after modification of the PEI with SDM used as a crosslinker. Moreover, it is understandable that PSOAT is entirely different from the polymer–lipid hybrid system and it is composed of low MW linear PEI, degradable ester linkages and also possesses abundant hydroxyl groups in the structure which significantly make the transporter less toxic.

3.3. Osmolarity of PSOAT

Osmotic activity is one of the key properties of the PSOAT system, which correlates with most of its functional properties including transfection efficacy or gene silencing capacity. We evaluated the osmotic properties of PSOAT using an automatic cryoscopic osmometer and compared it to that of D-sorbitol (a prime osmolyte used as a control) at various percentages. The osmolarity of PSOAT increased from 281 to 484 mOsm with increasing polysorbitol weight percentage from 1 to 5, in a manner similar to that of D-sorbitol (Table 1), suggesting that PSOAT has osmotic properties, which increases in a polysorbitol dose-dependent manner.

3.4. Silencing studies

At present, the therapeutic potential of using siRNA for targeted gene silencing is severely limited due to the lack of an effective delivery platform. Herein, we report a PSOAT system as an effective transporter of siRNA for efficient gene silencing. To test the silencing capability of the transporter, we examined luciferase and GFP silencing in A549 cells using siLuc and siGFP, respectively.

3.4.1. Luciferase silencing

Luciferase-expressing cells were transfected with siLuc or siScr using PSOAT and silencing by siLuc was compared against siScr treatment. The results demonstrated that the naked siLuc was completely ineffective as it exhibited no silencing. This is most likely because naked siRNAs cannot be transported through the cellular membrane [7]. On the other hand, an accelerated and remarkable silencing (>90%) was achieved through the transporter-mediated delivery of siLuc, which was 1.2-fold better than 'state-of-the-art' PEI 25K-mediated luciferase silencing (Fig. 4A). To note, nonspecific siScr exhibited negligible silencing, as expected. To verify that the improved PSOAT-mediated gene silencing was not affected by cellular toxicity, we performed a cell viability assay and found no perceptible toxicity of the PSOAT/siLuc complexes (Fig. S1). These results reveal the superior silencing efficacy of our PSOAT system.

3.4.2. GFP silencing

The silencing ability of PSOAT was further examined by flow cytometry analysis after transfection with siGFP in A549 cells. PSOAT/siGFP exhibited >90% GFP silencing, whereas siScr showed minimal silencing efficacy (Fig. 4B). The fluorescent microscopic images showed that a few cells expressed fluorescence when treated with PSOAT/siGFP, whereas the siScr group showed a level similar to that of the control. These results clearly demonstrate the enhanced gene silencing efficiency of our PSOAT system, facilitating an effective alternative carrier for siRNA transportation. This motivated us to investigate its RNAi-based silencing capability using another siRNA for therapeutic purpose.
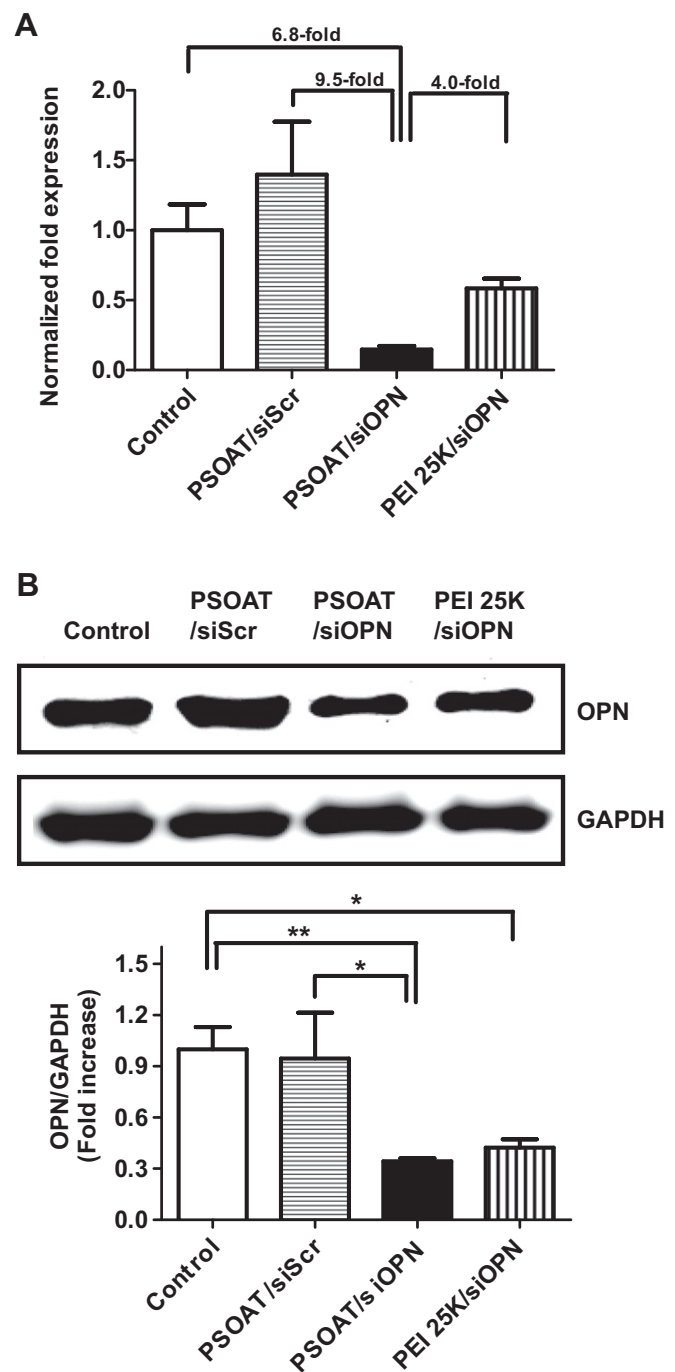
Fig. 5. Silencing of OPN expression through PSOAT and PEI 25K-mediated delivery of siOPN in A549 cells. Cells (80% confluence) were transfected with PSOAT/siOPN and PEI 25K/siOPN complexes and examined for OPN expression silencing efficacy by (A) RT-qPCR analysis, and (B) Western blot assay. Data are expressed as the mean ± SEM from three independent experiments, and representative bands are shown. The significance was analyzed using paired t-test; *$P < 0.05$ and **$P < 0.01$, respectively.

3.4.3. OPN silencing

We examined the effect of PSOAT on the delivery of a therapeutic OPN siRNA (siOPN) to suppress OPN expression. OPN is an acidic, adhesive, secreted glycophosphoprotein that has multiple functions related to tumorigenesis. The upregulated expression of OPN has been observed in a variety of cancers and is linked with tumor metastasis, relating to a poor prognosis for patients [39,40]. Therefore, the suppression of OPN could be a critical application
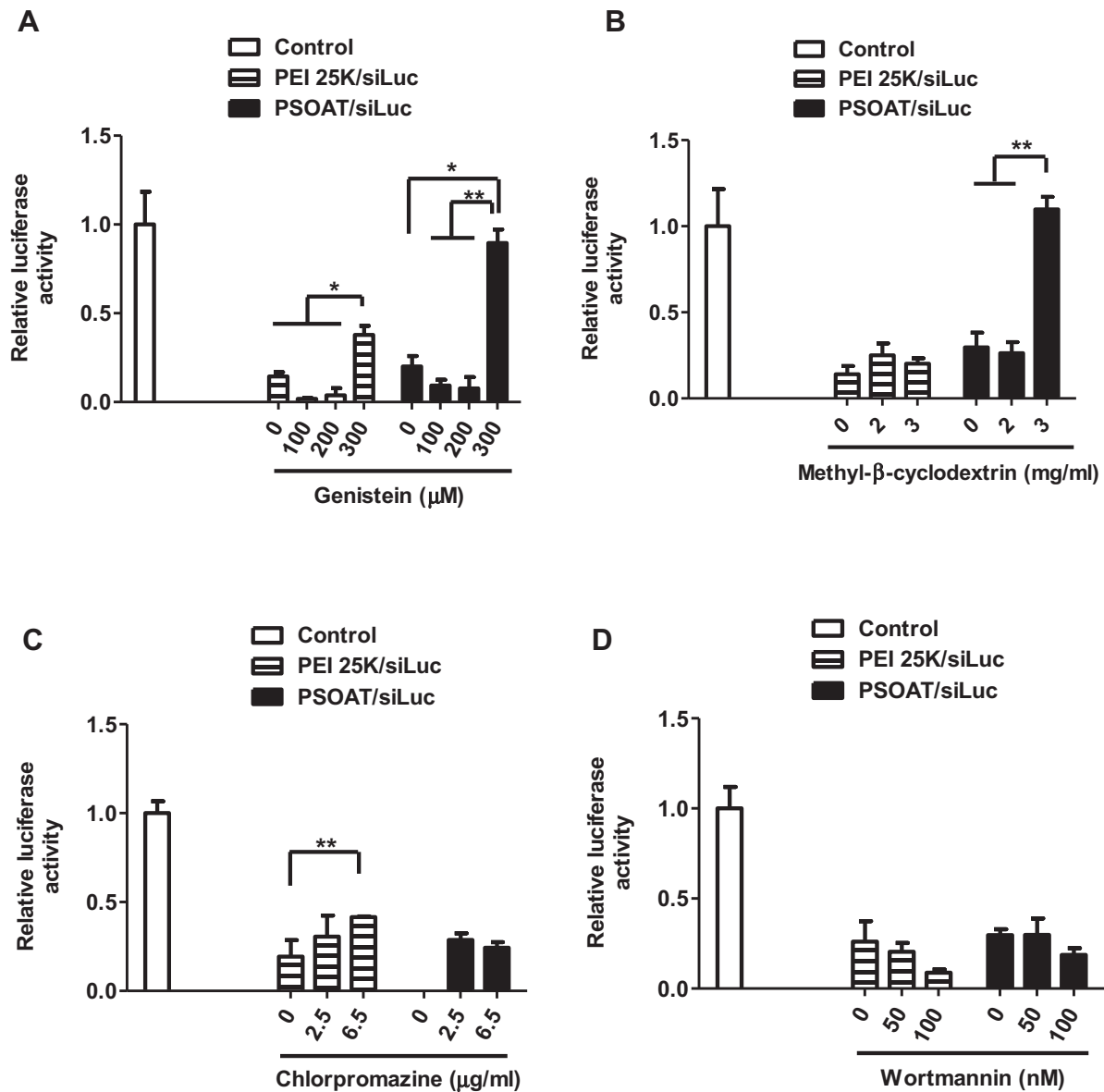
Fig. 6. Effect of various endocytosis inhibitors on PSOAT/siLuc-mediated cellular uptake and luciferase silencing in A549 cells. A549 cells (80% confluence) were incubated with (A) Genistein (GE), (B) Methyl-β-cyclodextrin (MβC), (C) Chlorpromazine (CH), and (D) Wortmannin (Wor) at various concentrations. Cells were then transfected with PSOAT/siLuc and PEI 25K/siLuc complexes in the presence of the inhibitors and the luciferase assay was performed ($n = 3$, error bar represents SD) (*$P < 0.05$; **$P < 0.01$; ***$P < 0.001$, one-way ANOVA).

where the use of siRNA technology has enormous potential. Thus, A549 cells were transfected with PSOAT/siOPN complexes and the silencing efficacy was analyzed by RT-qPCR and Western blotting. A remarkable suppression of OPN mRNA expression was observed with PSOAT/siOPN treatment, by about 10-fold and 4.5-fold compared to siScr- and PEI 25K-mediated silencing, respectively (Fig. 5A). The suppression of OPN through PSOAT was further confirmed by determining the OPN protein level by Western blot analysis. The results revealed significant siOPN silencing by PSOAT compared to the controls (Fig. 5B). It was obvious that the PSOAT system exhibited silencing effects that were superior to the standard PEI 25K.

The overexpression of OPN is involved in several other important signaling steps in cancer progression [41–44]. OPN expression promotes prostate cancer cell progression through the regulation of Akt/β-catenin [41] and Erk1/2 [42] activation, important steps in cancer progression. It is also strongly related to autotoxin (ATX)

expression in liver and human gastric cancer [43,44]. These studies seem to suggest the intimate co-regulation of OPN overexpression and various signaling mechanisms mostly in relation with cancer progression. The findings of the current study support the excellent potential of PSOAT as a promising candidate and a delivery vehicle for RNAi-mediated OPN suppression.

Taken together, silencing studies have shown markedly enhanced suppression of target genes using various siRNAs through PSOAT. At this stage, we were interested in investigating the precise mechanism involved in the acceleration of PSOAT-mediated siRNA transfection and gene silencing.

3.5. Mechanism of osmotic PSOAT in accelerated gene silencing

3.5.1. Cellular uptake mechanism and uptake selectivity

To further evaluate the mechanism of cellular uptake of the PSOAT/siRNA complexes, we utilized four different cellular uptake
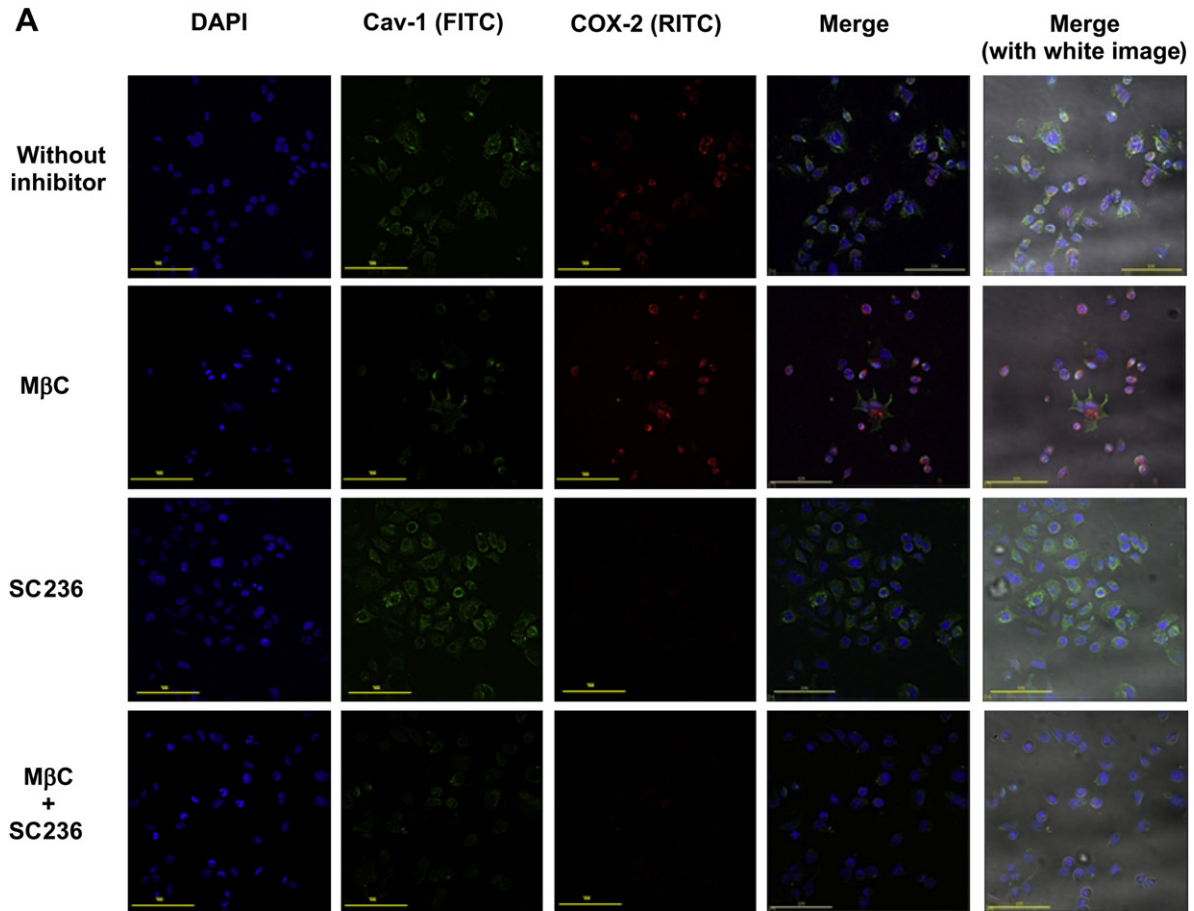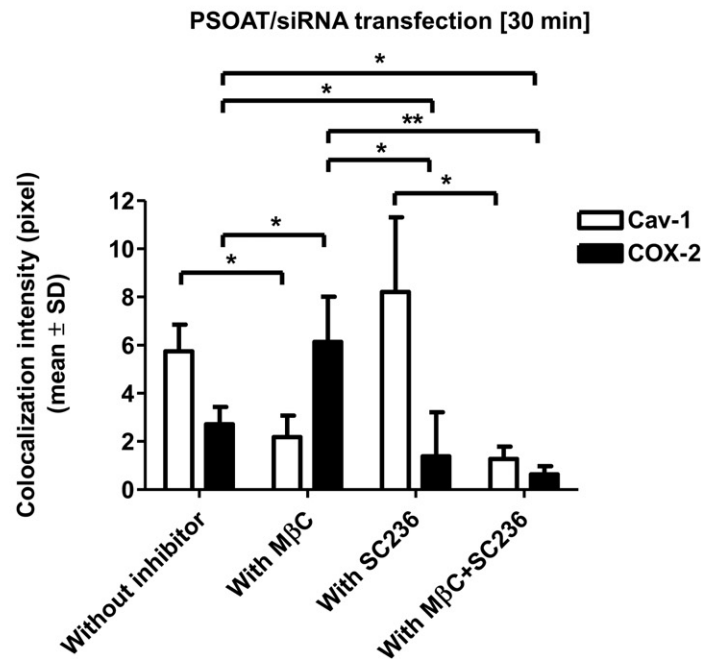
Fig. 7. Colocalization of Cav-1 and COX-2 after 30 min of PSOAT/siRNA-mediated transfection in the absence or presence of caveolae inhibitor (MβC) and/or COX-2 inhibitor (SC236) in A549 cells. (A) Cells were first incubated in the absence or presence of MβC or SC236 or MβC + SC236 for 1 h and transfected with PSOAT/siRNA complexes for 30 min in the presence of the inhibitor(s). The cell samples were treated with monoclonal mouse Cav-1 (1:50) and polyclonal rabbit COX-2 (1:50) IgG antibodies, and then incubated with anti-mouse FITC (for Cav-1) and anti-rabbit RITC (for COX-2)-conjugated secondary antibodies after fixation. Finally, samples were observed through image restoration microscopy (magnification: 20×) after being treated with DAPI containing fluoroshield solution. At least 1000 cells were examined in each experiment. Bar denotes 100 μm. (B) The colocalization graph was quantitatively plotted using measurements of intensity obtained through ImageJ software (NIH, USA). The white and black bars represent the colocalization of Cav-1 and COX-2, respectively, and are expressed as the mean pixel value ($n = 3$, error bar represents SD) (*$P < 0.05$; **$P < 0.01$, one-way ANOVA).
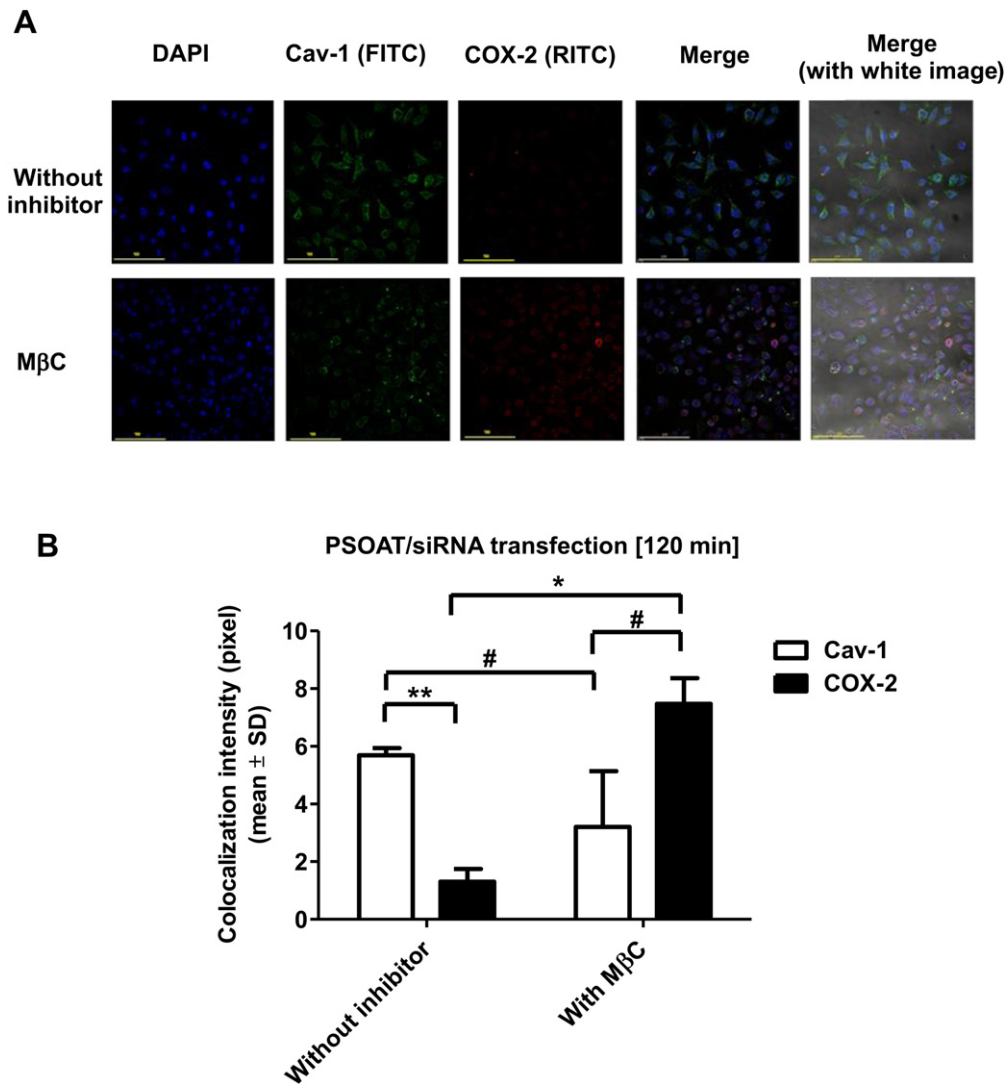
Fig. 8. Colocalization of Cav-1 and COX-2 at 120 min post-transfection by PSOAT/siRNA complexes in the absence or presence of caveolae inhibitor (MβC) in A549 cells. (A) Cells were first treated without or with MβC for 1 h and transfected with PSOAT/siRNA complexes for 120 min in the presence of inhibitor. Cells were treated with monoclonal mouse Cav-1 (1:50) and polyclonal rabbit COX-2 (1:50) IgG antibodies and then further treated with anti-mouse FITC (for Cav-1) and anti-rabbit RITC (for COX-2)-conjugated secondary antibodies after fixation. Finally, samples were observed through image restoration microscopy (magnification: 20×) after being treated with DAPI containing fluoroshield solution. At least 1000 cells were examined in each experiment. Bar denotes 100 μm. (B) The colocalization graph was quantitatively plotted using measurement of intensity obtained using ImageJ software (NIH, USA). The white and black bars represent the colocalization of Cav-1 and COX-2, respectively, and are expressed as the mean pixel value ($n = 3$, error bar represents SD) ($^{#}P < 0.1$, $^{*}P < 0.05$, $^{**}P < 0.01$, one-way ANOVA).

inhibitors including genistein (GE) and methyl-β-cyclodextrin (MβC) to inhibit caveolae-specific endocytosis, chlorpromazine (CH) as an inhibitor of clathrin-dependent endocytosis, and wortmannin (Wor) as a fluid-phase uptake inhibitor [26]. Because the high concentrations of these inhibitors could cause toxic side-effects, the concentrations were optimized by evaluating their cellular toxicity by MTT assay (data not shown). To probe the specific uptake mechanism, A549 cells expressing luciferase were transfected with PSOAT/siLuc complexes in the presence of inhibitors. Luciferase activity was calculated after normalization with siLuc-untreated control cells expressing luciferase (Fig. 6). PSOAT-mediated luciferase silencing was completely inhibited in the presence of GE and MβC inhibitors. On the other hand, no effects on gene silencing were observed with CH and Wor, suggesting that the cellular uptake of PSOAT/siLuc complexes and the silencing mechanism of PSOAT occur specifically via caveolae-mediated endocytosis. Note that, the PEI 25K-based luciferase silencing was affected significantly by the presence of both GE (300 μM) and CH (at all concentrations

investigated), demonstrating its non-selective endocytosis mechanism. No inhibition of the silencing effect was observed with MβC, whereas Wor slightly enhanced luciferase silencing by PEI 25K.

Hypertonic cells may block several uptake pathways including clathrin-dependent endocytosis and fluid-phase uptake [45,46], suggesting the existence of another cellular uptake mechanism in addition to the clathrin-dependent pathway under osmotic stress. Indeed, hypertonic exposure selectively stimulates caveolae-mediated endocytosis by downregulating clathrin-dependent and fluid-phase endocytosis [24]. Considering these facts, it appears that the hyperosmotic PSOAT selectively induced caveolae-mediated endocytosis due to its osmotic active polysorbitol backbone. Consequently, enhanced gene silencing was achieved through PSOAT-mediated delivery of siRNA, as evidenced by the specific inhibition of caveolae-mediated endocytosis. Our results and those of others have demonstrated that caveolae-mediated endocytosis of nanoparticles is an intracellular route, which is not hindered by lysosomal degradation and leads the internalized materials onto
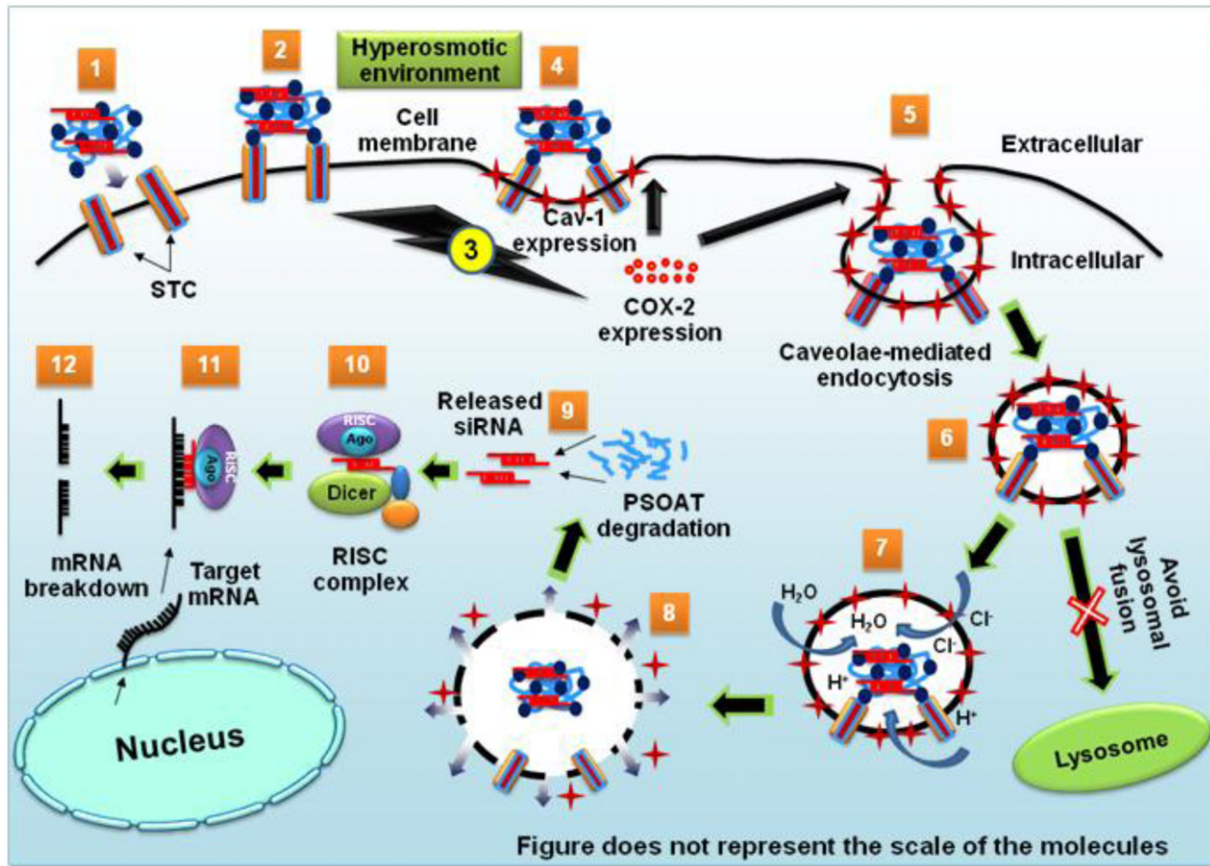
Fig. 9. Schematic representation on the function of PSOAT. Graphical presentation shows selective caveolae-mediated endocytosis of the PSOAT/siRNA complex following hyperosmotic pressure that induces Cav-1 and COX-2 expression, which accelerates the efficacy of the transporter for RNAi silencing. (1–2) PSOAT/siRNA complex recognizes and binds to the sorbitol transporting channel (STC) on the extracellular membrane and creates a hyperosmotic environment. (3–5) The osmotic pressure-sensitive PSOAT/siRNA complex induces caveolin (Cav)-1 expression and selectively stimulates caveolae-mediated endocytosis. This event subsequently generates COX-2 expression under osmotic stress. At this stage, Cav-1 expression augments and a mature caveolae structure is formed where COX-2 might work on disrupting the joint surface of particle deposition and accelerate caveolae-mediated endocytosis. (6) Selective caveolae endocytosis allows the PSOAT/siRNA complex containing caveolae endosome (caveosome) to avoid lysosomal fusion. (7–8) The endosome containing PSOAT/siRNA complex swells and eventually bursts due to the proton sponge effect of LPEI, which allows the complex to escape into the cytosol. (9) Due to the nature of degradable linkages, PSOAT degradation occurs and siRNAs are released. (10–12) The released siRNA recognizes and breaks down the target mRNA at the post-transcriptional level through an RNAi mechanism. Figure does not represent the scale of the molecules.

a non-acidic and non-digestive pathway [16]. In contrast, clathrin-dependent endocytosis follows the classic endocytic route, which cannot avoid lysosomal fusion, and thus causes the degradation of the internalized particles [16]. Therefore, the current study further elucidates the benefits of PSOAT with selective caveolae-mediated internalization to achieve accelerated silencing efficacy of RNAi.

3.5.2. Effects of COX-2 on PSOAT-mediated gene silencing

Our previous study demonstrated the inhibition of PSOAT-mediated gene transfection by SC236, a COX-2-specific inhibitor [10]. This finding led us to hypothesize that COX-2 might be involved in the acceleration of PSOAT-based cellular internalization. Therefore, to validate the involvement of COX-2 in PSOAT/siRNA-mediated gene silencing, we examined the silencing efficacy using the SC236 inhibitor at various concentrations. Luciferase silencing was completely inhibited by PSOAT/siLuc in the presence of 20 μM SC236, whereas PEI 25K/siLuc exhibited no such effect (Fig. S2), suggesting that COX-2 might play a role in the acceleration of PSOAT-mediated gene silencing due to the high osmotic properties of the transporter. Recent studies have also reported the hypertonicity-dependent regulation of COX-2 in association with osmolyte-dependent (e.g., sorbitol-dependent) adaptation of cells under hyperosmotic conditions [29,30]. Moreover, cells with high COX-2 expression display increased cellular uptake than cells with low COX-2 expression [31], indicating that osmotic-active PSOAT/siLuc complexes might induce COX-2 expression which may in turn synergistically affect the enhanced cellular uptake of the particles, resulting in accelerated gene silencing.

The induction of COX-2 expression under osmotic stimuli is regulated through the activation of epidermal growth factor receptor (EGFR) or mitogen-activated protein kinase (MAPK)

signaling (especially p38 and ERK 1/2) [47,48]. Under osmotic stimuli, metalloproteinase (MMP) activates MAPK through MMP-dependent EGFP ligands including EGF, HB-EGF, and TGF-α, which could establish membrane-associated osmosensing complexes for COX-2 expression [49]. These COX-2, MMPs, and adhesion molecules under osmotic stimuli can enhance cellular uptake by degrading the site of the joint surface of particle deposition on the cell membrane, leading to accelerated infiltration via endocytosis [50]. So far, we have found that PSOAT selectively induces caveolae-mediated endocytosis for cellular uptake and that the acceleration of PSOAT-mediated gene silencing may involve COX-2; this could help us investigate any synergistic involvement of caveolae endocytosis together with COX-2 expression and action of COX-2 in the acceleration of this endocytosis mechanism.

3.5.3. Involvement of Cav-1 and COX-2 in PSOAT-mediated gene silencing

Caveolin-1 (Cav-1) expression is essential for caveolae formation [25,27]. Caveolae are flask-shaped invaginations of the plasma membrane coated by Cav-1, which is indispensable for the regulation of caveolae-mediated endocytosis [26]. Osmotic stress-induced increase of caveolae-mediated endocytosis is associated with Cav-1 expression and its translocation from the plasma membrane [24]. Thus, we examined the expression of Cav-1, as an indicator of caveolae-dependent endocytosis, and COX-2 in A549 cells after transfection with PSOAT/siRNA at 15, 30, 60, and 120 min. Minimal changes in Cav-1 expression were observed in cells treated with PSOAT/siRNA complexes, similar to untreated controls at 15 min post-transfection; however, the expression was increased after 30 min and continued to increase gradually up to 120 min, as illustrated in Fig. S3. On the other hand, COX-2 expression was also increased at 30 min post-transfection; however, it decreased dramatically at 60 min post-transfection (Fig. S4). Then we asked whether Cav-1 regulates COX-2 expression after PSOAT-mediated transfection. Several reports have described Cav-1-mediated suppression or degradation of COX-2 protein [51,52]. Rodriguez et al. showed the suppression of COX-2 by Cav-1 through a β-catenin-Tcf/Lef-dependent transcriptional pathway by alleviation of prostaglandin E2 and survivin [51]. On the other hand, Chen et al. demonstrated that Cav-1 binding at the carboxy (C)-terminal region of COX-2 in endoplasmic reticulum (ER) facilitated its degradation [52]. Our results suggest that both Cav-1 and COX-2 are expressed after PSOAT-mediated transfection and involved in accelerating the cellular internalization of PSOAT complexes where COX-2 works at the initial phase after transfection, however, Cav-1 might interact with COX-2 later on and facilitate the downregulation of it. Based on a previous report that the depletion of Cav-1 induces increased COX-2 [52], we used MβC as an inhibitor of caveolae formation, thus the downregulation of Cav-1 expression was used to confirm the possible interaction of Cav-1 and COX-2 following PSOAT/siRNA transfection. The results from the colocalization study demonstrated the induction of Cav-1 and COX-2 expression after 30 min of transfection in the absence of inhibitor, further suggesting the involvement of both Cav-1 and COX-2 in PSOAT-mediated gene silencing, as shown in Fig. 7. However, the expression of Cav-1 was markedly reduced, which allowed the significant increase in COX-2 expression in the presence of MβC, revealing the possible interaction between them. Moreover, the results showed significant decreases of COX-2 or both Cav-1 and COX-2 in the presence of SC236 or MβC plus SC236, respectively. On the other hand, a minimal level of COX-2 was colocalized with an increased level of Cav-1 at 120 min post-transfection of POSAT/siRNA without inhibitor (Fig. 8). Interestingly, when the expression of Cav-1 was reduced in the presence of MβC, COX-2 expression was significantly elevated, further supporting the idea of an interaction between Cav-1 and

COX-2. It should be noted that the cells treated with D-sorbitol, a prime osmolyte, exhibited a similar phenomenon for Cav-1 and COX-2 expression and revealed their possible interaction, as shown in Fig. S5, suggesting that PSOAT exerted its accelerated silencing mechanism in relation with Cav-1 and COX-2 expression due to its hyperosmotic polysorbitol backbone. Our results suggest that the expression of Cav-1 induced by PSOAT/siRNA plays an important role in caveolae-mediated endocytosis together with COX-2. Furthermore, COX-2 during the initial-phase of transfection might accelerate endocytosis resulting in effective gene silencing. A schematic illustration of the overall concept is depicted in Fig. 9. To the best of our knowledge, this is the first demonstration of the synergistic functional involvement of selective caveolae-mediated endocytosis and COX-2 expression for accelerated RNAi-mediated gene silencing through a non-viral gene carrier system.

4. Conclusion

PSOAT displayed promising siRNA transport potential for effective gene silencing. The excellent siRNA complexation and protection against degradative enzymes, effective physicochemical properties of PSOAT/siRNA complexes with reduced toxicity, and accelerated silencing efficacy make PSOAT remarkably efficient as a siRNA carrier system. Moreover, we demonstrated the impressive efficacy of this transporter for the delivery of therapeutic siOPN *in vitro*, suggesting the application of this transporter system to prevent OPN-related tumorigenesis. Our mechanistic studies demonstrated that PSOAT advantageously shifts the route of cellular uptake to the selective caveolae-mediated endocytic pathway and it is functionalized via Cav-1 and COX-2 expression for advanced cellular internalization, suggesting a selective uptake mechanism with controlled intracellular fate and selective stimulation of signaling molecules through PSOAT, which ensured accelerated silencing. Although a few mechanisms such as the overall interaction between Cav-1 and COX-2 and the detailed feasibility of COX-2-triggered acceleration of caveolae-mediated endocytosis will require further investigation, the mechanism revealed in the present study will allow us to design a potent non-viral siRNA carrier for effective and targeted silencing with advanced efficacy. Further studies of the *in vivo* efficacy of PSOAT with the advanced functional mechanism using therapeutic siRNA are underway.

Appendix A. Supplementary data

Supplementary data related to this article can be found at http://dx.doi.org/10.1016/j.biomaterials.2012.08.049.

References

[1] Fire A, Xu S, Montgomery MK, Kostas SA, Driver SE, Mello CC. Potent and specific genetic interference by double-stranded RNA in *Caenorhabditis elegans*. Nature 1998;391:806–11.
[2] Elbashir SM, Lendeckel W, Tuschl T. RNA interference is mediated by 21- and 22-nucleotide RNAs. Genes Dev 2001;15:188–200.

[3] Elbashir SM, Harborth J, Lendeckel W, Yalcin A, Weber K, Tuschl T. Duplexes of 21-nucleotide RNAs mediate RNA interference in cultured mammalian cells. Nature 2001;411:494–8.

[4] McCaffrey AP, Meuse L, Pham TTT, Conklin DS, Hannon GJ, Kay MA. Gene expression − RNA interference in adult mice. Nature 2002;418:38–9.

[5] Leuschner F, Dutta P, Gorbatov R, Novobrantseva TI, Donahoe JS, Courties G, et al. Therapeutic siRNA silencing in inflammatory monocytes in mice. Nat Biotechnol 2011;29:1005–10.

[6] Love KT, Mahon KP, Levins CG, Whitehead KA, Querbes W, Dorkin JR, et al. Lipid-like materials for low-dose, in vivo gene silencing. Proc Natl Acad Sci U S A 2010;107:1864–9.

[7] Whitehead KA, Langer R, Anderson DG. Knocking down barriers: advances in siRNA delivery. Nat Rev Drug Discov 2009;8:129–38.

[8] Kleinman ME, Yamada K, Takeda A, Chandrasekaran V, Nozaki M, Baffi JZ, et al. Sequence- and target-independent angiogenesis suppression by siRNA via TLR3. Nature 2008;452:591–7.

[9] Bitko V, Musiyenko A, Shulyayeva O, Barik S. Inhibition of respiratory viruses by nasally administered siRNA. Nat Med 2005;11:50–5.

[10] Islam MA, Yun CH, Choi YJ, Shin JY, Arote R, Jiang HL, et al. Accelerated gene transfer through a polysorbitol-based transporter mechanism. Biomaterials 2011;32:9908–24.

[11] Ma M, Li F, Yuan ZF, Zhuo RX. Influence of hydroxyl groups on the biological properties of cationic polymethacrylates as gene vectors. Acta Biomater 2010; 6:2658–65.

[12] Park MR, Han KO, Han IK, Cho MH, Nah JW, Choi YJ, et al. Degradable polyethylenimine-alt-poly(ethylene glycol) copolymers as novel gene carriers. J Control Release 2005;105:367–80.

[13] Khalil IA, Kogure K, Akita H, Harashima H. Uptake pathways and subsequent intracellular trafficking in nonviral gene delivery. Pharmacol Rev 2006;58: 32–45.

[14] Rejman J, Conese M, Hoekstra D. Gene transfer by means of lipo- and poly-plexes: role of clathrin and caveolae-mediated endocytosis. J Liposome Res 2006;16:237–47.

[15] Le Roy C, Wrana JL. Clathrin- and non-clathrin-mediated endocytic regulation of cell signalling. Nat Rev Mol Cell Biol 2005;6:112–26.

[16] Ferrari A, Pellegrini V, Arcangeli C, Fittipaldi A, Giacca M, Beltram F. Caveolae-mediated internalization of extracellular HIV-1 tat fusion proteins visualized in real time. Mol Ther 2003;8:284–94.

[17] Pelkmans L, Helenius A. Endocytosis via caveolae. Traffic 2002;3:311–20.

[18] Chung YC, Cheng TY, Young TH. The role of adenosine receptor and caveolae-mediated endocytosis in oligonucleotide-mediated gene transfer. Biomaterials 2011;32:4471–80.

[19] Dokka S, Rojanasakul Y. Novel non-endocytic delivery of antisense oligonu-cleotides. Adv Drug Deliv Rev 2000;44:35–49.

[20] Rejman J, Bragonzi A, Conese M. Role of clathrin- and caveolae-mediated endocytosis in gene transfer mediated by lipo- and polyplexes. Mol Therapy 2005;12:468–74.

[21] Ding HM, Ma YQ. Role of physicochemical properties of coating ligands in receptor-mediated endocytosis of nanoparticles. Biomaterials 2012;33:5798–802.

[22] Ding HM, Tian WD, Ma YQ. Designing nanoparticle translocation through membranes by computer simulations. Acs Nano 2012;6:1230–8.

[23] Yang K, Ma YQ. Computer simulation of the translocation of nano-particles with different shapes across a lipid bilayer. Nat Nanotechnol 2010;5:579–83.

[24] Wang SH, Singh RD, Godin L, Pagano RE, Hubmayr RD. Endocytic response of type I alveolar epithelial cells to hypertonic stress. Am J Physiol Lung Cell Mol Physiol 2011;300:L560–8.

[25] Drab M, Verkade P, Elger M, Kasper M, Lohn M, Lauterbach B, et al. Loss of caveolae, vascular dysfunction, and pulmonary defects in caveolin-1 gene-disrupted mice. Science 2001;293:2449–52.

[26] Iversen TG, Skotland T, Sandvig K. Endocytosis and intracellular transport of nanoparticles: present knowledge and need for future studies. Nano Today 2011;6:176–85.

[27] Razani B, Engelman JA, Wang XB, Schubert W, Zhang XL, Marks CB, et al. Caveolin-1 null mice are viable but show evidence of hyperproliferative and vascular abnormalities. J Biol Chem 2001;276:38121–38.

[28] Volonte D, Galbiati F, Pestell RG, Lisanti MP. Cellular stress induces the tyro-sine phosphorylation of caveolin-1 (Tyr(14)) via activation of p38 mitogen-activated protein kinase and c-Src kinase − evidence for caveolae, the actin cytoskeleton, and focal adhesions as mechanical sensors of osmotic stress. J Biol Chem 2001;276:8094–103.

[29] Moeckel GW, Zhang L, Fogo AB, Hao CM, Pozzi A, Breyer MD. COX2 activity promotes organic osmolyte accumulation and adaptation of renal medullary interstitial cells to hypertonic stress. J Biol Chem 2003;278:19352–7.

[30] Yang TX, Huang YN, Heasley LE, Berl T, Schnermann JB, Briggs JP. MAPK mediation of hypertonicity-stimulated cyclooxygenase-2 expression in renal medullary collecting duct cells. J Biol Chem 2000;275:23281–6.

[31] Yang DJ, Bryant J, Chang JY, Mendez R, Oh CS, Yu DF, et al. Assessment of cyclooxygense-2 expression with 99mTc-labeled celebrex. Anti-cancer Drugs 2004;15:255–63.

[32] Kiss AL, Botos E. Endocytosis via caveolae: alternative pathway with distinct cellular compartments to avoid lysosomal degradation? J Cell Mol Med 2009; 13:1228–37.

[33] Du XL, Jiang T, Sheng XG, Gao R, Li QS. Inhibition of osteopontin suppresses in vitro and in vivo angiogenesis in endometrial cancer. Gynecol Oncol 2009; 115:371–6.

[34] Kumar V, Behera R, Lohite K, Karnik S, Kundu GC. p38 Kinase is crucial for osteopontin-induced furin expression that supports cervical cancer progres-sion. Cancer Res 2010;70:10381–91.

[35] Mok H, Lee SH, Park JW, Park TG. Multimeric small interfering ribonucleic acid for highly efficient sequence-specific gene silencing. Nat Mater 2010;9:272–8.

[36] Barreto JA, O'Malley W, Kubeil M, Graham B, Stephan H, Spiccia L. Nanomaterials: applications in cancer imaging and therapy. Adv Mater 2011;23:H18–40.

[37] Ryser HJP. A membrane effect of basic polymers dependent on molecular size. Nature 1967;215:934–6.

[38] Schroeder A, Dahlman JE, Sahay G, Love KT, Jiang S, Eltoukhy AA, et al. Alkane-modified short polyethyleneimine for siRNA delivery. J Control Release 2012; 160:172–6.

[39] Bhattacharya SD, Garrison J, Guo HT, Mi ZY, Markovic J, Kim VM, et al. Micro-RNA-181a regulates osteopontin-dependent metastatic function in hepato-cellular cancer cell lines. Surgery 2010;148:291–7.

[40] Zhang AM, Liu Y, Shen YZ, Xu YH, Li XT. Osteopontin silencing by small interfering RNA induces apoptosis and suppresses invasion in human renal carcinoma Caki-1 cells. Med Oncol 2010;27:1179–84.

[41] Robertson BW, Chellaiah MA. Osteopontin induces beta-catenin signaling through activation of Akt in prostate cancer cells. Exp Cell Res 2010;316:1–11.

[42] Robertson BW, Bonsal L, Chellaiah MA. Regulation of Erk1/2 activation by osteopontin in PC3 human prostate cancer cells. Mol Cancer 2010;9:260.

[43] Zhang RH, Wang J, Ma SJ, Huang ZH, Zhang GX. Requirement of osteopontin in the migration and protection against taxol-induced apoptosis via the ATX-LPA axis in SGC7901 cells. BMC Cell Biol 2011;12:11.

[44] Zhang RH, Zhang ZH, Pan XL, Huang XY, Huang ZH, Zhang GX. ATX-LPA axis induces expression of OPN in hepatic cancer cell SMMC7721. Anat Rec 2011; 294:406–11.

[45] Daukas G, Zigmond SH. Inhibition of receptor-mediated but not fluid-phase pinocytosis in polymorphonuclear leukocytes. J Cell Biol 1985;101:1673–9.

[46] Heuser JE, Anderson RGW. Hypertonic media inhibit receptor-mediated endocytosis by blocking clathrin-coated pit formation. J Cell Biol 1989;108: 389–400.

[47] Kuper C, Bartels H, Fraek ML, Beck FX, Neuhofer W. Ectodomain shedding of pro-TGF-alpha is required for COX-2 induction and cell survival in renal medullary cells exposed to osmotic stress. Am J Physiol Cell Physiol 2007;293: C1971–82.

[48] Zhao HY, Tian W, Tai C, Cohen DM. Hypertonic induction of COX-2 expression in renal medullary epithelial cells requires transactivation of the EGFR. Am J Physiol Renal Physiol 2003;285:F281–8.

[49] Kuper C, Steinert D, Fraek ML, Beck FX, Neuhofer W. EGF receptor signaling is involved in expression of osmoprotective TonEBP target gene aldose reductase under hypertonic conditions. Am J Physiol Renal Physiol 2009;296:F1100–8.

[50] O'Neill KD, Chen NX, Wang M, Cocklin R, Zhang Y, Moe SM. Cellular uptake of beta2M and AGE-beta2M in synovial fibroblasts and macrophages. Nephrol Dial Transplant 2003;18:46–53.

[51] Rodriguez DA, Tapia JC, Fernandez JG, Torres VA, Munoz N, Galleguillos D, et al. Caveolin-1-mediated suppression of cyclooxygenase-2 via a beta-catenin-Tcf/Lef-dependent transcriptional mechanism reduced prostaglandin E2 produc-tion and survivin expression. Mol Biol Cell 2009;20:2297–310.

[52] Chen SF, Liou JY, Huang TY, Lin YS, Yeh AL, Tam K, et al. Caveolin-1 facilitates cyclooxygenase-2 protein degradation. J Cellular Biochem 2010;109:356–62.